Molecular Biology of the Cell
Vol. 11, 4205–4216, December 2000

Endosome to Golgi Transport of Ricin Is Regulated by Cholesterol

Stine Grimmer,* Tore-Geir Iversen,* Bo van Deurs,† and Kirsten Sandvig*‡

*Institute for Cancer Research, The Norwegian Radium Hospital, Montebello, 0310 Oslo, Norway; †Structural Cell Biology Unit, Department of Medical Anatomy, The Panum Institute, University of Copenhagen, DK-2200 Copenhagen N, Denmark

Submitted August 18, 2000; Revised October 4, 2000; Accepted October 11, 2000
Monitoring Editor: Hugh R.B. Pelham

We have here studied the role of cholesterol in transport of ricin from endosomes to the Golgi apparatus. Ricin is endocytosed even when cells are depleted for cholesterol by using methyl-β-cyclodextrin (mβCD). However, as here shown, the intracellular transport of ricin from endosomes to the Golgi apparatus, measured by quantifying sulfation of a modified ricin molecule, is strongly inhibited when the cholesterol content of the cell is reduced. On the other hand, increasing the level of cholesterol by treating cells with mβCD saturated with cholesterol (mβCD/chol) reduced the intracellular transport of ricin to the Golgi apparatus even more strongly. The intracellular transport routes affected include both Rab9-independent and Rab9-dependent pathways to the Golgi apparatus, since both sulfation of ricin after induced expression of mutant Rab9 (mRab9) to inhibit late endosome to Golgi transport and sulfation of a modified mannose 6-phosphate receptor (M6PR) were inhibited after removal or addition of cholesterol. Furthermore, the structure of the Golgi apparatus was affected by increased levels of cholesterol, as visualized by pronounced vesiculation and formation of smaller stacks. Thus, our results indicate that transport of ricin from endosomes to the Golgi apparatus is influenced by the cholesterol content of the cell.

INTRODUCTION

During the last few years, it has become clear that cholesterol plays an essential role in endocytosis and intracellular sorting. Recently it has been shown that cholesterol is necessary for the invagination of clathrin-coated pits (Rodal *et al*., 1999; Subtil *et al*., 1999). By removing cholesterol from the plasma membrane with methyl-β-cyclodextrin (mβCD), the clathrin-coated pits are unable to form invaginations, and thereby the clathrin-dependent endocytosis is strongly reduced. Also, it is well known that the structure of invaginated caveolae is strictly dependent on cholesterol (Rothberg *et al*., 1990; Schnitzer *et al*., 1994; Hailstones *et al*., 1998). On the other hand, clathrin-independent endocytosis in several cell lines is largely unaffected by cholesterol depletion (Rodal *et al*., 1999).

‡ Corresponding author. E-mail address: ksandvig@radium.uio.no.

Abbreviations used: mRab9, Rab9 mutant; M6PR, mannose 6-phosphate receptor; M6PR46HMY, 46-kDa cation-dependent mannose 6-phosphate receptor tagged with polyhistidine, c-myc epitope, and tyrosine sulfation site; mβCD, methyl-β-cyclodextrin; mβCD/chol, methyl-β-cyclodextrin saturated with cholesterol; ricin sulf-2, ricin A-sulf-2 chain reconstituted with ricin B-chain.

Cholesterol and cholesterol-containing microdomains are also known to be involved in intracellular transport. In the genetic disorder Niemann-Pick type C, cholesterol accumulates in late endosomes (Mukherjee and Maxfield, 1999). This accumulation leads to a redistribution of membrane proteins and an impairment of late endosome to Golgi transport of the lysosomal enzyme receptor IGF2/MPR (Mukherjee and Maxfield, 1999; Kobayashi *et al*., 1999). Furthermore, elevated cholesterol levels in normal fibroblasts can inhibit transport of the fluorescent analogue of the glycosphingolipid lactosylceramide to the Golgi apparatus, a similar phenotype as seen in sphingolipid-storage diseases (Puri *et al*., 1999). The transport of glycosyl-phosphatidylinositol-anchored proteins and transmembrane proteins to the apical side of polarized cells is also dependent on cholesterol (Keller and Simons, 1998; Mayor *et al*., 1998). In this respect, cholesterol is associated with sphingolipids forming rafts, which are thought to associate with specific proteins while excluding others (Harder and Simons, 1997; Simons and Ikonen, 1997; Benting *et al*., 1999).

Cellular proteins like furin and TGN38 are transported from the cell surface to the Golgi apparatus, presumably by different pathways (Ghosh *et al*., 1998; Mallet and Maxfield, 1999). Furthermore, a number of protein toxins are transported to the Golgi apparatus on their way to the cytosol

(Olsnes *et al*., 1993; Sandvig and van Deurs, 1996). To what extent transport of different proteins to the Golgi apparatus is dependent on cholesterol has not been investigated. We here wanted to study the involvement of cholesterol in the endosome to Golgi transport of the protein toxin ricin. Ricin is a plant toxin which consists of an enzymatically active A-chain and a B-chain responsible for cell binding and subsequent intracellular transport. The toxin binds to glycolipids and glycoproteins with terminal galactose at the cell surface, and it is endocytosed by both clathrin-dependent and clathrin-independent mechanisms (Sandvig and van Deurs, 1996, 1999). After endocytosis, most of the toxin is either recycled or transported through the endosomal system to lysosomes, while a fraction is transported to the Golgi apparatus (van Deurs *et al*., 1986, 1988). Recent data indicate that ricin can be transported to the Golgi apparatus by a Rab9-independent process, presumably circumventing late endosomes (Iversen, Llorente, Nicoziani, van Deurs, and Sandvig, unpublished data). From the Golgi apparatus, ricin is transported retrogradely to the ER before translocation to the cytosol where it exerts its cytotoxic effect (Wales *et al*., 1993; Simpson *et al*., 1995; Wesche *et al*., 1999). Since ricin is endocytosed even when the clathrin-dependent mechanism is turned off by removal of cholesterol from the cell surface (Rodal *et al*., 1999), the toxin can serve as a marker to investigate the effect of cholesterol removal on intracellular transport.

In the present article, we have studied the effect of cholesterol on the endosome to Golgi transport. To alter the cholesterol levels, we have used mβCD to extract cholesterol from the plasma membrane, and mβCD saturated with cholesterol (mβCD/chol) to insert cholesterol into the plasma membrane. We here show that the level of cholesterol in the cell strongly influences the endosome to Golgi transport, and that increased cholesterol concentration leads to fragmentation of the Golgi apparatus.

MATERIALS AND METHODS

Materials

mβCD (average degree of substitution, 10.5–14.7 methyl groups per molecule), cholesterol, HEPES, geneticin, puromycin, lactose, ricin, ricin B-chain, holo-transferrin (iron-saturated), aprotinin, PMSF, and monensin were obtained from Sigma Chemical Co. (St. Louis, MO). [^{3}H]leucine and $Na_2{}^{35}SO_4$ were obtained from Amersham Pharmacia Biotech (Amersham, Buckinghamshire, UK). Na[^{125}I] was purchased from DuPont (Brussels, Belgium). Protein A-sepharose was purchased from Pharmacia (Sweden). Ricin and transferrin were ^{125}I-labeled according to Fraker and Speck (1978) to a specific activity of 2×10^4–6×10^4 cpm/ng. Ricin B-chain was labeled with Cy3 (Amersham Life Science, Inc., IL) according to the instructions given by the supplier. A monovalent conjugate of ricin B-chain coupled covalently to HRP was prepared as described earlier (van Deurs *et al*., 1986). We employed 5 mM of mβCD and mβCD/chol in order to avoid any toxic effects of mβCD.

Cells and Cell Culture

The HeLa-TetOn/Rab9 S21N cell line transfected with mutant Rab9 (mRab9) (Iversen, Llorente, Nicoziani, van Deurs, and Sandvig, unpublished data) was maintained in DMEM (Flow Laboratories, Irvine, Scotland) supplemented with 5% FCS (Life Technologies, Paisly, Scotland), 100 μg/ml streptomycin, 100 U/ml penicillin, 2 mM L-glutamine (Life Technologies), 0.2 mg/ml geneticin and 0.5 μg/ml puromycin. The HeLa-TetOn/Rab9/M6PR46HMY cell line was maintained in the same medium supplemented with 200 μg/ml zeocin (CAYLA, France).

If not otherwise stated, the HeLa-TetOn/Rab9 S21N cell line was used without expression of the mRab9.

Preparation of mβCD Saturated with Cholesterol

The saturated complex was mainly prepared as previously described (Klein *et al*., 1995). Thirty milligrams of cholesterol were added to 1 g of mβCD dissolved in 20 ml H_2O. The mixture was rotated overnight at 37°C, and the resulting clear solution was freeze-dried. The complex was stored at room temperature.

Measurement of Endocytosis

Endocytosed ^{125}I-labeled transferrin was measured after 5 min at 37°C as the percentage of total cell-associated (endocytosed and surface-bound) transferrin as described earlier (Ciechanover *et al*., 1983).

Endocytosed ^{125}I-labeled ricin was measured after 15 min and 2 h at 37°C as the amount of toxin that could not be removed with lactose as previously described (Sandvig and Olsnes, 1979).

In both instances, the cells were preincubated with 5 mM mβCD or mβCD/chol for 30 min at 37°C.

Cholesterol Determination

Cell monolayers were washed carefully with PBS, lysed in a buffer containing 0.1% SDS, 1 mM Na_2EDTA and 0.1 M Tris-HCl, pH 7.4, and homogenized using a 19-gauge needle attached to a 1-ml syringe. The cholesterol content was determined enzymatically by the use of a cholesterol assay kit (Sigma, St. Louis, MO).

Protein Determination

The protein content of the homogenized cells was measured using the micro bicinchoninic acid method (Pierce, Rockford, IL) according to the manufacturer's instructions.

Sulfation of Ricin A-sulf-2

Ricin A-sulf-2, modified to contain a tyrosine sulfation site and three partially overlapping N-glycosylation sites, was produced, purified and reconstituted with ricin B chain (ricin sulf-2) as previously described (Rapak *et al*., 1997). The cells were washed in sulfate-free DME medium (Flow Laboratories, Irvine, Scotland) supplemented with 2 mM L-glutamine, 1× nonessential amino acids (Life Technologies) and 1 mM $CaCl_2$, and incubated with 0.2 mCi/ml $Na_2{}^{35}SO_4$ in the same medium for 4 h. Then mβCD or mβCD/chol was added to a final concentration of 5 mM, and the cells incubated further for 30 min before addition of ricin sulf-2 (~200 ng/ml). After 2 h, the medium was removed and the cells were washed twice for 5 min with 0.1 M lactose in HEPES at 37°C followed by cold PBS. The cells were then lysed (lysis buffer: 0.1 M NaCl, 10 mM Na_2HPO_4, 1 mM EDTA, 1% Triton X-100, 0.1 mM PMSF and 1.5 μg/ml aprotinin, pH 7.4), and centrifuged to remove nuclei for 10 min at 5,000 rpm at 4°C in an Eppendorf centrifuge. The supernatant was immunoprecipitated overnight at 4°C with rabbit antiricin antibodies immobilized on protein A-sepharose. Finally, the beads were washed twice with cold PBS containing 0.35% Triton X-100, and the absorbed material was analyzed by SDS-PAGE (12%) under reducing conditions.

Measurement of Ricin Cytotoxicity

The cells were washed twice with HEPES medium lacking leucine and then incubated with the same medium containing 5 mM mβCD or mβCD/chol. After 30 min, increasing toxin concentrations were added and the cells incubated further for 2 h. The cells were then

incubated in HEPES medium containing 1 μCi/ml [^{3}H]leucine for 15 min at 37°C, extracted with 5% TCA for 10 min, followed by brief washing in 5% TCA, and subsequently dissolved in 0.1 M KOH. The cell-associated radioactivity was then measured.

Sulfation of Mannose-6-Phosphate-Receptor

The assay was performed essentially as described by Itin *et al*. (1997).

Accumulation of Unsulfated MPR46HMY. The HeLa-TetOn/Rab9/M6PR46HMY cell line was cultured for 3 d to subconfluency in a modified sulfate-free DME medium (added 1× MEM amino acids (Life Technologies), 1× nonessential amino acids, 2 mM L-glutamine, 100 μg/ml streptomycin, 100 U/ml penicillin, 1× vitamin solution (Life Technologies), 1 mM sodium pyruvate (Flow Laboratories), 200 mg/ml $CaCl_2$ containing 7.5% FCS, and 10 mM Na-chlorate. The medium was changed daily.

[^{35}S]Sulfate Labeling and Purification of M6PR46HMY. The cells were washed twice with DME medium without sulfate, and incubated for 30 min with 5 mM mβCD or mβCD/chol in the modified sulfate-free SMEM medium (as above). One millicurie per milliliter $Na_2{}^{35}SO_4$ was then added, and the cells were incubated further for 2 h. The cells were then washed once with PBS and solubilized in RIPA buffer (50 mM Tris/HCl, pH 7.8, 150 mM NaCl, 1% sodium deoxycholate, 0.1% SDS, 1.5% Triton X-100) supplemented with 0.1 mM PMSF, 1.5 μg/ml aprotinin, and 25 mM imidazole. Insoluble material was pelleted in an Eppendorf centrifuge at 14,000 rpm for 10 min at 4°C. The M6PR46-HMY receptors were purified by adding prewashed nickel agarose beads (Ni-NTA, Qiagen, Inc.) to the cleared lysate and incubating the suspension by rotation for 2 h at 4°C. The precipitate was washed four times with RIPA supplemented with 25 mM imidazole, and the receptors were eluted with the same buffer supplemented with 25 mM EDTA. The eluted material was analyzed by SDS-PAGE (12%) under reducing conditions.

SDS-PAGE

SDS-PAGE was carried out as described earlier (Laemmli, 1970). The gels were fixed in 4% acetic acid and 27% methanol for 30 min, and then treated with 1 M sodium salicylate, pH 5.8, in 2% glycerol for 20 min. Dried gels were exposed to Kodak XAR-5 films (Rochester, NY) at − 80°C for fluorography.

Recycling and Degradation of Ricin

The cells were washed twice with HEPES medium and then incubated with the same medium containing 5 mM mβCD or mβCD/chol at 37°C. After 30 min, ^{125}I-labeled ricin was added and the cells incubated further for 20 min. Excess ricin associated with the cell surface was then removed by washing the cells four times with 0.1 M lactose in HEPES at 37°C during a 5-min period. Finally, the recycling and degradation of ricin was measured after 2-h incubation in the presence of 1 mM lactose as the amount of toxin that could either be pelleted from the medium or remained in the supernatant.

Confocal Microscopy

Cells grown on coverslips were washed twice with HEPES medium and incubated with 5 mM mβCD or mβCD/chol for 30 min at 37°C. Cy3-labeled ricin B-chain (1,000 ng/ml) was then added, and the cells incubated further for 2 h at 37°C before fixation. The cells were fixed with 3% paraformaldehyde in PBS for 15 min in room temperature, and permeabilized with 0.1% Triton X-100 in PBS for 5 min. To label the Golgi apparatus, the cells were incubated with either rabbit antimannosidase II antibodies (provided by Dr. Kelley Moremen, University of Georgia, Athens, GA) or sheep antihuman TGN46 (Serotec, Oxford, UK) in PBS containing 5% FCS followed by either fluorescein isothiocyanate-labeled goat antirabbit IgG (Jackson Immunoresearch, West Grove, PA) or fluorescein isothiocyanate-labeled donkey antisheep/goat IgG (Serotec, Oxford, UK) in PBS containing 5% FCS. After staining, the coverslips were mounted in Mowiol (Calbiochem, San Diego, CA). Confocal microscopy was performed with the use of a Leica (Wetzlar, Germany) confocal microscope. Images were taken at ×63 magnification and captured as images at 1,024 × 1,024 pixels. Montages of images were prepared with the use of Photoshop 4.0 (Adobe, Mountain View, CA).

Table 1. The cholesterol content in micrograms per milligram protein after 30 min, 60 min, and 2.5 h incubation with 5 mM mβCD or mβCD/chol

Treatment	Cholesterol after 30 min[a]	Cholesterol after 60 min[a]	Cholesterol after 2.5 h[a]
Control	27 ± 4 (100%)	26 ± 2 (100%)	23 ± 4 (100%)
5 mM mβCD	20 ± 2 (74%)	17 ± 4 (65%)	13 ± 4 (58%)
5 mM mβCD/chol	48 ± 5 (178%)	54 ± 7 (208%)	58 ± 9 (256%)

[a] Sterol mass is expressed as microgram per milligram of cell protein, and the data are means ± SD from three independent assays each performed in duplicate.

Electron Microscopy

The cells were washed twice with HEPES medium and preincubated with 5 mM mβCD or mβCD/chol for 30 min at 37°C before addition of a monovalent conjugate of ricin B-chain coupled covalently to HRP (Sigma type IV). After incubating the cells further for 2 h at 37°C, they were washed with PBS, and fixed with 2% glutaraldehyde in 0.1 M cacodylate buffer, pH 7.2, for 60 min at room temperature. The cells were then carefully washed with PBS (five times) and incubated in PBS containing 0.5 mg/ml diaminobenzidine and 0.5 μl/ml a 30% H_2O_2 solution for 60 min at room temperature. The cells were then washed, scraped off the flasks, pelleted, and postfixed with OsO_4, contrasted en block with 1% uranyl acetate, dehydrated in a graded series of ethanols, and embedded in Epon. Sections were further contrasted with lead citrate and uranyl acetate and examined in a Phillips CM 100 electron microscope (Phillips, Eindhoven, the Netherlands).

RESULTS

Effect of mβCD and mβCD/chol on Endocytosis of Ricin and Transferrin

In this study, we wanted to investigate the importance of cholesterol for transport of ricin from endosomes to the Golgi apparatus. To change the cholesterol level in the cells, we used mβCD and mβCD/chol. While treatment with 5 mM mβCD reduced the cholesterol content of the cells by nearly 25% after 30 min, treating the cells with 5 mM mβCD/chol increased the cholesterol content by 75% (Table 1). The amount of cholesterol removed or added increased upon further incubation.

We first investigated the effect of increased and decreased cholesterol levels on endocytosis in the HeLa-TetOn/Rab9 S21N cell line where mRab9 expression can be induced. The cells were pretreated with 5 mM mβCD or mβCD/chol for 30 min in order to extract or insert cholesterol, before the

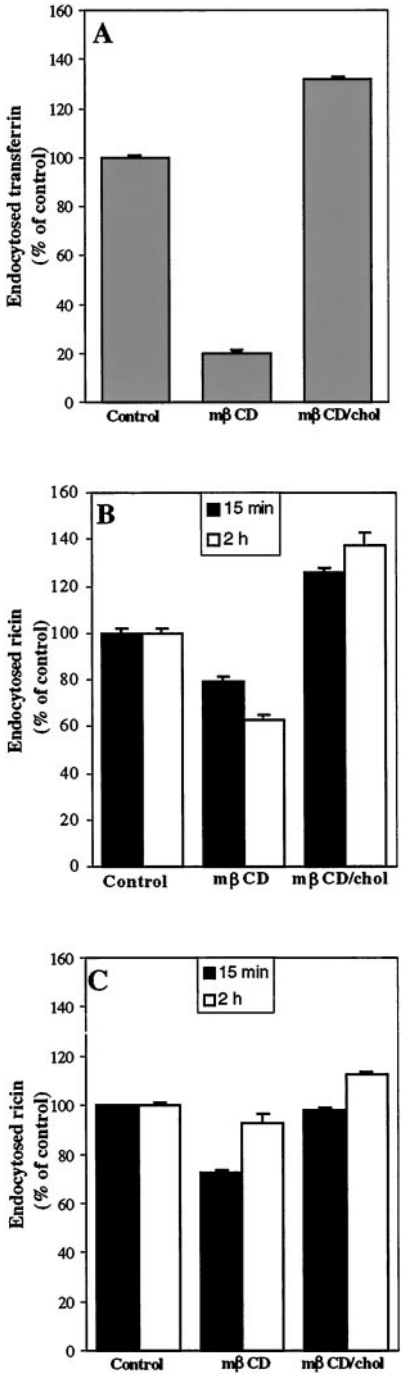

Figure 1. Effect of mβCD and mβCD/chol on endocytosis of transferrin (A) and ricin in the absence (B) and presence of monensin (5 μM) (C). The HeLa-TetOn/Rab9S21N cells were washed twice in HEPES medium and incubated with or without 5 mM mβCD and mβCD/chol for 30 min at 37°C before ^{125}I-labeled transferrin or ^{125}I-labeled ricin were added to the cells. The amounts of endocytosed transferrin was measured after 5 min, while the amounts of endocytosed ricin was measured after 15 min and 2 h as described in Material and Methods. The error bars show deviations between duplicates of a typical experiment.

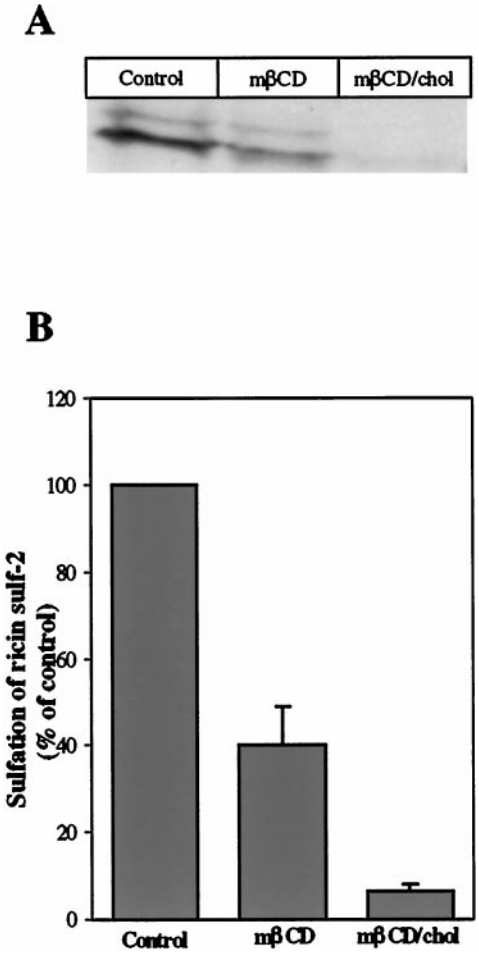

Figure 2. Effect of mβCD and mβCD/chol on sulfation of ricin sulf-2. (A) Representative example of the resulting bands seen after fluorography in a given experiment. The HeLa-TetOn/Rab9S21N cells were washed with sulfate-free DME medium and incubated for 4 h in the presence of $Na_2{}^{35}SO_4$ before addition of 5 mM mβCD or mβCD/chol. After 30 min, ricin sulf-2 was added, and the incubation continued for 2 h. The cells were then washed with 0.1 M lactose in HEPES medium at 37°C and with ice-cold PBS before they were lysed. The nuclei were removed by centrifugation, and the sulfated ricin was immunoprecipitated with rabbit antiricin antibodies attached to protein A-sepharose overnight at 4°C. The immunoprecipitate was analyzed by SDS-PAGE (12%) under reducing conditions followed by fluorography. The intensities of the resulting bands were determined by densiometric quantitation using ImageQuant 5.0. (B) Averaged data of three independent experiments.

endocytosis of transferrin and ricin was measured. Ricin endocytosis was measured both after 15 min and 2 h. As shown in Figure 1, mβCD (5 mM) had a strong effect on endocytosis of transferrin in this cell line, reducing it by nearly 80% (Figure 1A). Ricin endocytosis was only reduced by ~20% after 15 min, but after 2 h the amount of endocytosed ricin was reduced by 40% (Figure 1B). On the other hand, treatment with mβCD/chol increased both the endocytosis of transferrin and ricin with ~20–40% as compared with control cells (Figure 1A and B). To see whether the

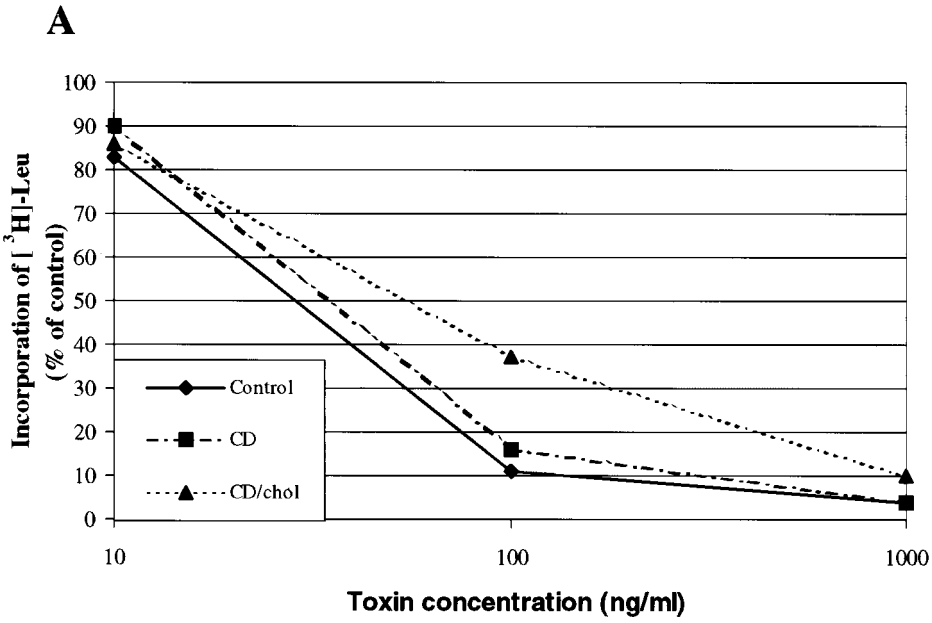

B

Summary from 4 experiments		
	Average Protection	SD
5 mM mβCD	1.25	0.25
5 mM mβCD/chol	2.0	0.32

Figure 3. The effect of mβCD and mβCD/chol on the cytotoxicity of ricin in the HeLa-TetOn/Rab9S21N cell line. (A) Representative example of the toxic effect of increasing concentrations of ricin in a given experiment. (B) Averaged data of four independent experiments. The cells were washed twice with HEPES medium lacking leucine and incubated with or without 5 mM mβCD and mβCD/chol for 30 min at 37°C before increasing concentrations of ricin were added. After incubating the cells for 2 h, the toxic effect was measured as described in Material and Methods.

apparent decrease in endocytosis of ricin after 2 h was due to an increased degradation, endocytosis of ricin was also measured in the presence of monensin (5 μM) to decrease degradation. As shown (Figure 1C), this treatment prevented the apparent reduction of ricin endocytosis after 2 h in the presence of mβCD.

Removal and Addition of Cholesterol Inhibit Sulfation of Ricin

In order to measure the transport of ricin to the Golgi apparatus, we employed a modified ricin molecule with a tyrosine sulfation site (Rapak *et al*., 1997). Three glycosylation sites added to the A-chain make it possible to also follow transport of ricin to the ER (Rapak *et al*., 1997). The cells were incubated with $Na_2{}^{35}SO_4$ for at least 4 h before addition of 5 mM mβCD or mβCD/chol. After 30 min, ricin was added and the cells incubated further for 2 h before the sulfated forms of ricin were isolated and quantified as described in Material and Methods. Figure 2A shows that both in control cells and in cells treated with mβCD, two bands representing sulfated ricin appeared; the upper band represents sulfated ricin that was also glycosylated. Only one band was discernible for cells treated with mβCD/chol. Glycosylated ricin was not visible, possibly due to a low amount of the sulfated form. As the bands representing the glycosylated form of ricin were so weak, we only quantified the bands representing ricin that was only sulfated. The sulfation of ricin decreased with ~55% in the presence of mβCD, while treatment with mβCD/chol resulted in a ~95% decrease as compared with control cells (Figure 2B). This indicates a strong reduction in transport of ricin to the Golgi apparatus, especially after treatment with mβCD/chol. Interestingly, when the cells were treated with lower concentrations of mβCD/chol (0.5 mM and 1 mM) there was an increase in sulfation of ricin as compared with control cells. In contrast, ricin sulfation was gradually decreased with increasing concentrations of mβCD (0.5–5 mM) (our unpublished results). Control experiments showed that the sulfation of cellular proteins was not reduced to the same extent. Treatment with mβCD had no inhibitory effect, while mβCD/chol reduced the sulfation by ~45% (our unpublished results), which is much less than observed for ricin.

Cellular Cholesterol Affects the Cytotoxicity of Ricin

To further investigate whether retrograde transport of ricin was affected by treatment with mβCD and mβCD/chol, we performed a toxicity experiment. Little effect on the toxicity of ricin was seen after incubation with mβCD (Figure 3), as only 1.25 ± 0.25 (SD) times more toxin was required to obtain 50% reduction in protein synthesis. Following treatment with mβCD/chol, the cells were protected 2.0 ± 0.32

(SD) times against ricin (Figure 3). Thus, the protection seemed to be somewhat smaller than the reduction in sulfation.

Both Rab9-dependent and Rab9-independent Transport to the Golgi Is Affected by the Cholesterol Content

We have recently found that ricin can be transported to the Golgi apparatus by a Rab9-independent pathway (Iversen, Llorente, Nicoziani, van Deurs, and Sandvig, unpublished data), in agreement with the idea that there is a pathway to the Golgi apparatus circumventing late endosomes (Mallard *et al*., 1998; Ghosh *et al*., 1998; Mallet and Maxfield, 1999). We have here investigated whether both Rab9-independent and Rab9-dependent transport to the Golgi is affected by the cholesterol content of the membrane, by measuring sulfation of ricin in the presence of mRab9 to inhibit late endosome to Golgi transport (Iversen, Llorente, Nicoziani, van Deurs, and Sandvig, unpublished data) (Riederer *et al*., 1994) and by quantifying sulfation of a modified M6PR containing a tyrosine sulfation site (Itin *et al*., 1997). To examine the Rab9-independent pathway, we incubated the cells in the presence of doxycycline for 18 h in order to achieve maximal expression of the mRab9 (Iversen, Llorente, Nicoziani, van Deurs, and Sandvig, unpublished data), before the sulfation of ricin was performed as described in Materials and Methods. Also, in the presence of mRab9, addition of both mβCD and mβCD/chol reduced sulfation of ricin (Figure 4). The Rab9-dependent pathway was investigated by using the HeLa-TetOn/Rab9/M6PR46HMY cell line, which overexpress a modified M6PR with a sulfation site constitutively (Iversen, Llorente, Nicoziani, van Deurs, and Sandvig, unpublished data). To measure modification of the receptor with radioactive sulfate, it was necessary to accumulate a pool of unsulfated M6PR46HMY by growing the cells for 3 d in a sulfate-free medium containing chlorate to reversibly inhibit protein sulfation (Baeuerle and Huttner, 1986). The cells were then incubated with mβCD or mβCD/chol for 30 min before labeling the receptor with $^{35}SO_4^{2-}$. The sulfated M6PR46HMY was harvested as described in Material and Methods by means of a N-terminal polyhistidine tag that binds to the nickel resin and run on a 12% SDS-PAGE. Quantitation of the resulting bands (Figure 5) revealed that also sulfation of the M6PR was reduced to a similar extent as sulfation of ricin by removal or addition of cholesterol.

Effect of Cholesterol on other Pathways Taken by Ricin

To investigate if pathways other than endosome to Golgi transport were affected by the cholesterol content, we examined the effect of mβCD and mβCD/chol on the recycling and degradation of ricin. As shown in Figure 6, treatment with mβCD resulted in a slight decrease in the recycling of ricin, while the degradation increased by ~50%. On the other hand, mβCD/chol had no effect on the recycling of ricin, but decreased the amount of degraded ricin by ~40% as compared with control cells. Thus, the cholesterol content seems to affect these pathways to a somewhat lesser extent and to a certain degree in a different manner than what is observed for endosome to Golgi transport.

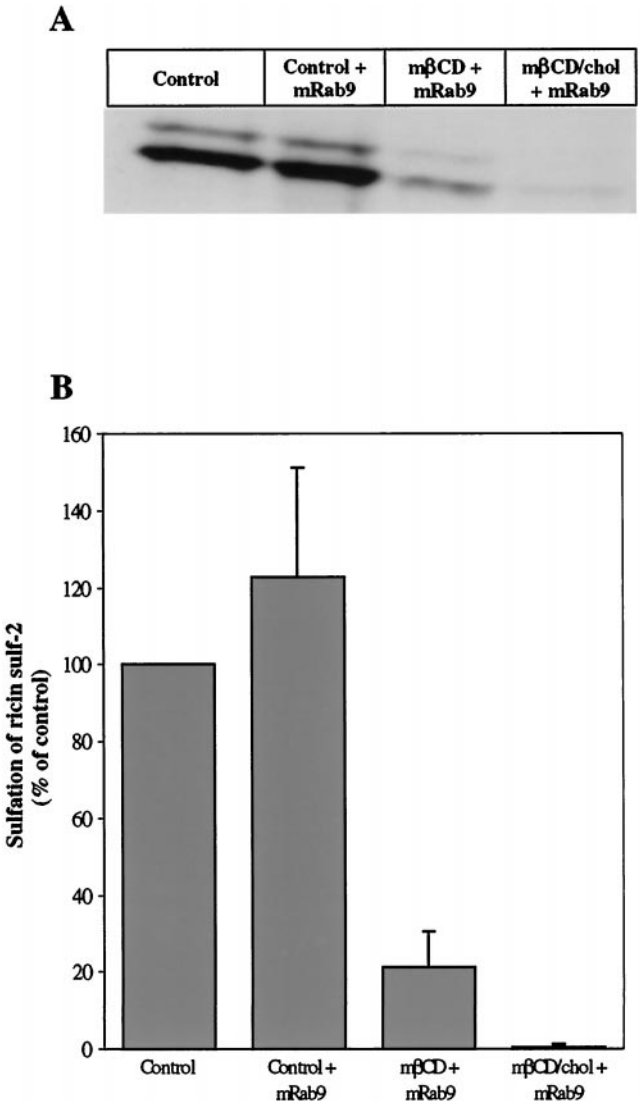

Figure 4. Effect of mβCD and mβCD/chol on the Rab9-independent pathways to the Golgi apparatus. (A) Representative example of the resulting bands seen after fluorography in a given experiment. The HeLa-TetOn/Rab9S21N cell line was grown with or without doxycycline (2μg/ml) for 18 h in order to express mRab9. The cells were then washed with sulfate-free DME medium, and incubated for 4 h in the presence of $Na_2{}^{35}SO_4$ before addition of 5 mM mβCD or mβCD/chol. After 30 min, ricin sulf-2 was added, and the incubation continued for 2 h. The sulfated ricin molecule was then harvested and analyzed as described in Materials and Methods. The intensities of the resulting bands were determined by densiometric quantitation using ImageQuant 5.0. (B) Summary from two independent experiments.

Increased Cholesterol Content Affects the Structure of the Golgi Apparatus

Having established that the intracellular transport to the Golgi apparatus is affected by variations of the cholesterol content, we wanted to look at the localization of ricin as well as the structure of the Golgi apparatus in order to see

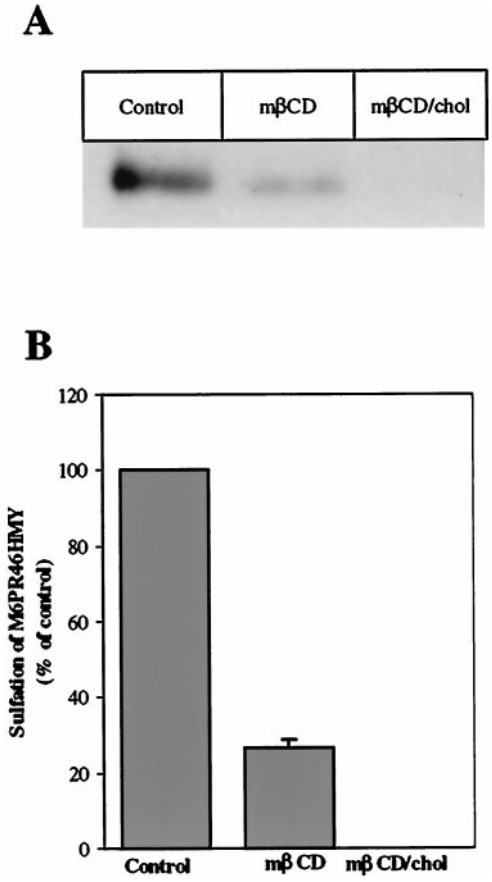

Figure 5. Effect of mβCD and mβCD/chol on the Rab9-dependent pathway to the Golgi apparatus. (A) Representative example of the resulting bands seen after fluorography in a given experiment. The HeLa-TetOn/Rab9/M6PR46HMY cell line was grown for 3 d in sulfate-free medium. The cells were then treated with 5 mM mβCD or mβCD/chol before labeling of the modified M6PR with $Na_2{}^{35}SO_4$ for 2 h. The sulfated receptor was harvested and analyzed as described in Materials and Methods. The intensities of the resulting bands were determined by densiometric quantitation using ImageQuant 5.0. (B) Summary from two independent experiments.

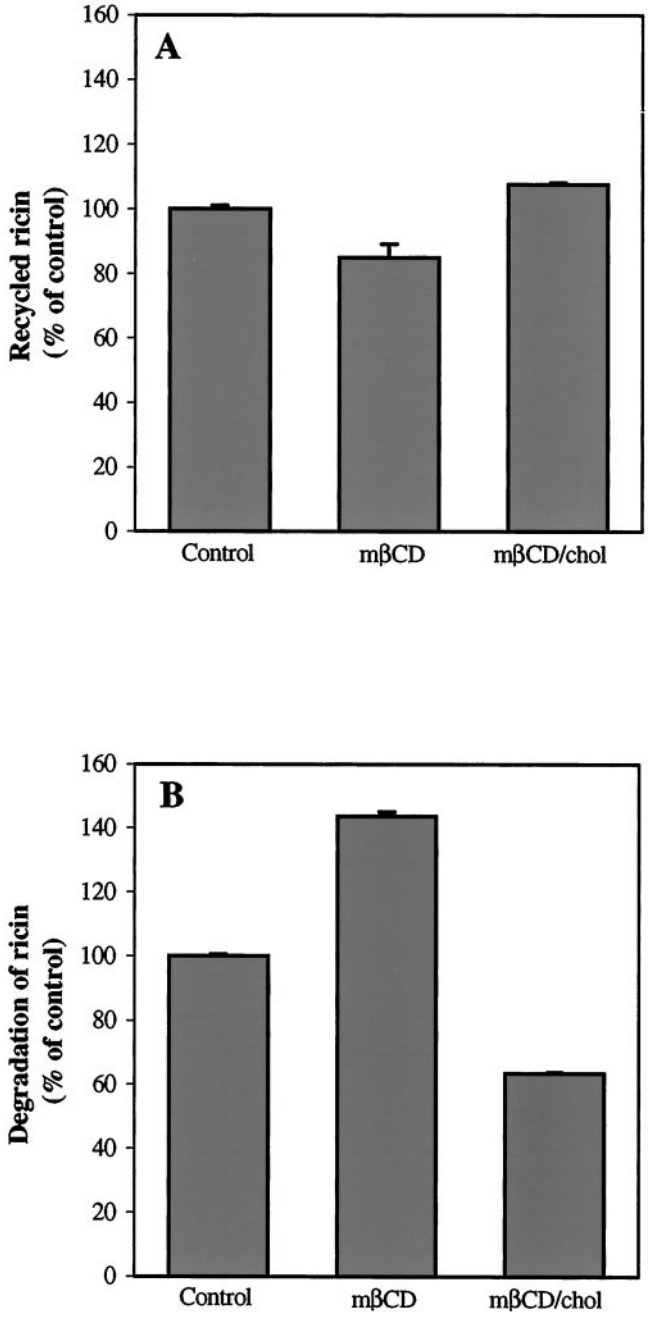

Figure 6. Effect of mβCD and mβCD/chol on the recycling (A) and degradation (B) of ricin in the HeLa-TetOn/Rab9S21N cell line. The cells were washed twice with HEPES medium, and incubated with or without 5 mM mβCD and mβCD/chol for 30 min at 37°C. ^{125}I-labeled ricin was then added, and the cells incubated further for 20 min before the amount of recycled and degraded ricin was measured as described in Material and Methods. The error bars show deviations between duplicates of a typical experiment.

whether any changes were discernible. We employed confocal microscopy using Cy3-labeled ricin B-chain to look at the ricin transport in order to avoid any toxic effect of ricin. To label the Golgi apparatus, we employed an antibody against mannosidase II as well as an antibody against TGN46. Both internalized ricin B-chain and the Golgi apparatus are clearly localized to the perinuclear region of the cell in control cells and cells treated with mβCD (Figure 7A, B, D, and E). However, mβCD treated cells also show a distinct peripheral Cy3 signal (Figure 7B and E), which may represent peripherally localized endosomes. In cells treated with mβCD/chol, ricin B-chain is still mainly localized to the perinuclear region, but the Golgi apparatus show a more dispersed pattern compared with control- and mβCD-treated cells (Figure 7C and F). This apparent fragmentation of the Golgi apparatus is visible already after 30 min incubation with mβCD/chol (our unpublished results). To study this in more detail, the localization of ricin B-chain was investigated by the electron microscope using a monovalent conjugate of ricin B-chain covalently coupled to HRP. In control cells, well-developed Golgi stacks were present, and

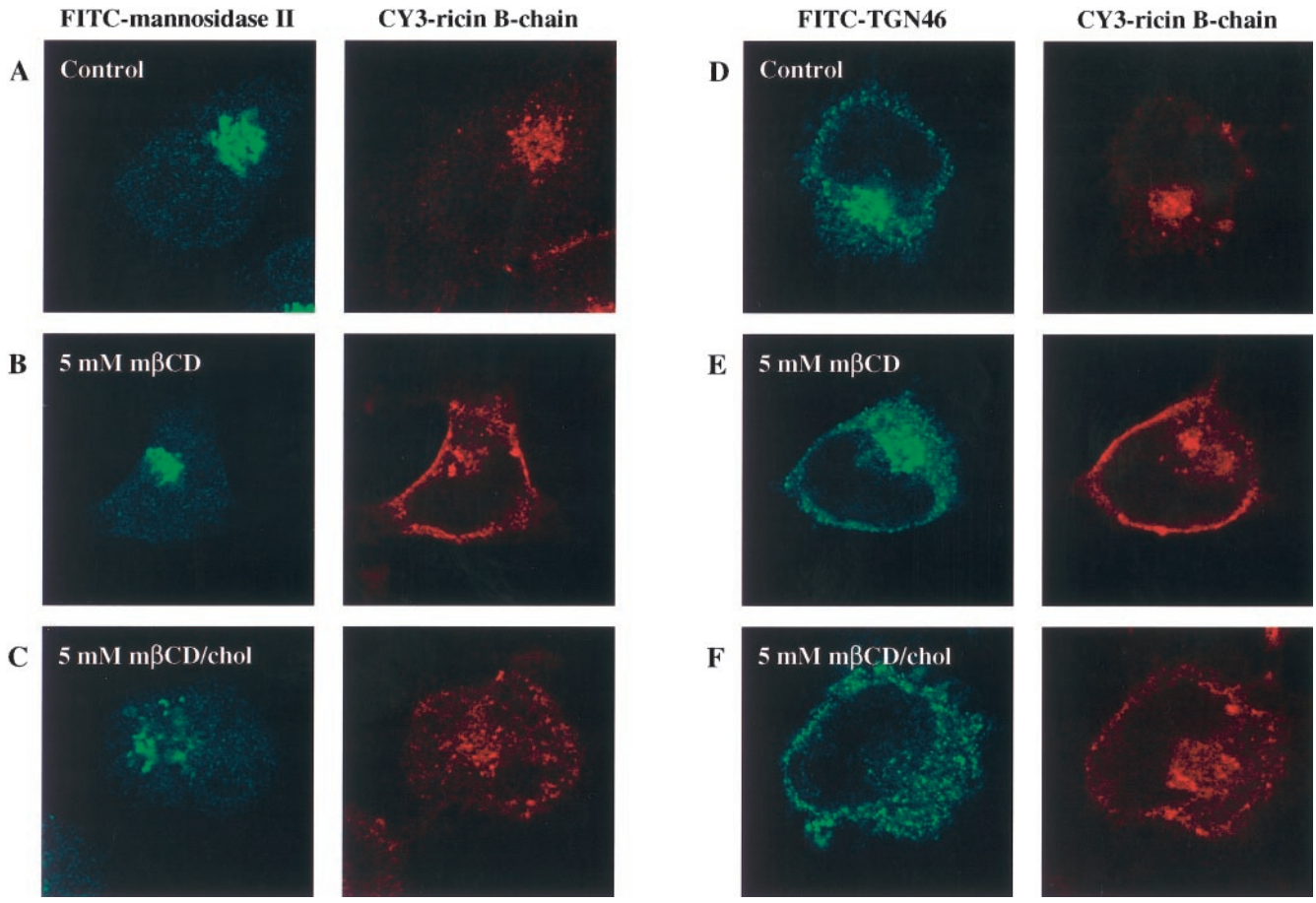

Figure 7. Effect of mβCD and mβCD/chol on the localization of Cy3-labeled ricin B-chain and the structure of the Golgi apparatus. The HeLa-TetOn/Rab9S21N cell line was treated with 5 mM of mβCD or mβCD/chol for 30 min at 37°C. Cy3-labeled ricin B-chain (1,000 ng/ml) was then added, and the incubation continued for 2 h. The cells were then fixed, permeabilized and stained with either an antibody against the Golgi marker mannosidase II (A to C) or an antibody against TGN46 (D to F).

ricin B-chain could be seen in the TGN as well as in endosomes and lysosomes (Figure 8A and B). Incubation with mβCD did not cause any marked changes in cell morphology or labeling pattern. However, following treatment with mβCD/chol, the appearance of the Golgi apparatus was dramatically changed (Figure 8C-F). The Golgi stacks were considerably smaller and less frequent than in control cells, and no structures reminiscent of the TGN and accessible to internalized ricin B-chain were observed. In the Golgi regions, however, numerous small (50–100 nm) vesicles had accumulated, some of which were labeled with ricin B-HRP (Figure 8C-F). Thus, an increased cholesterol content may affect the intracellular transport of ricin to the Golgi apparatus by affecting the structure of this organelle.

DISCUSSION

In the present study, we have investigated the influence of cholesterol on intracellular transport of ricin by using mβCD to selectively extract cholesterol from the plasma membrane and mβCD/chol to insert cholesterol. We have earlier shown that removal of cholesterol with mβCD inhibits clathrin-dependent endocytosis in a number of cell lines, while the clathrin-independent endocytosis is largely unaffected (Rodal *et al*., 1999). Here we show that the intracellular transport of ricin from endosomes to the Golgi apparatus is reduced by ~55% following treatment with mβCD, while reduction of ricin endocytosis is smaller. In this connection it is important to note that ricin endocytosed by clathrin-independent endocytosis reaches the Golgi apparatus and exhibits full toxic effect on the cells (Sandvig *et al*., 1987). Recycling of ricin was only slightly affected by mβCD treatment, while the degradation of ricin increased by nearly 40% following extraction of cholesterol. Our results also show that the intracellular transport of ricin to the Golgi apparatus is even more affected by treatment with mβCD/chol, which reduces the transport by ~95%. Again, this cannot be explained by a decreased endocytosis, as mβCD/chol increases the endocytosis of ricin after 2 h by nearly 40%. Furthermore, mβCD/chol has no effect on the recycling of ricin, while the degradation in this case is reduced by 35%. Interestingly, both confocal microscopy and electron micros-

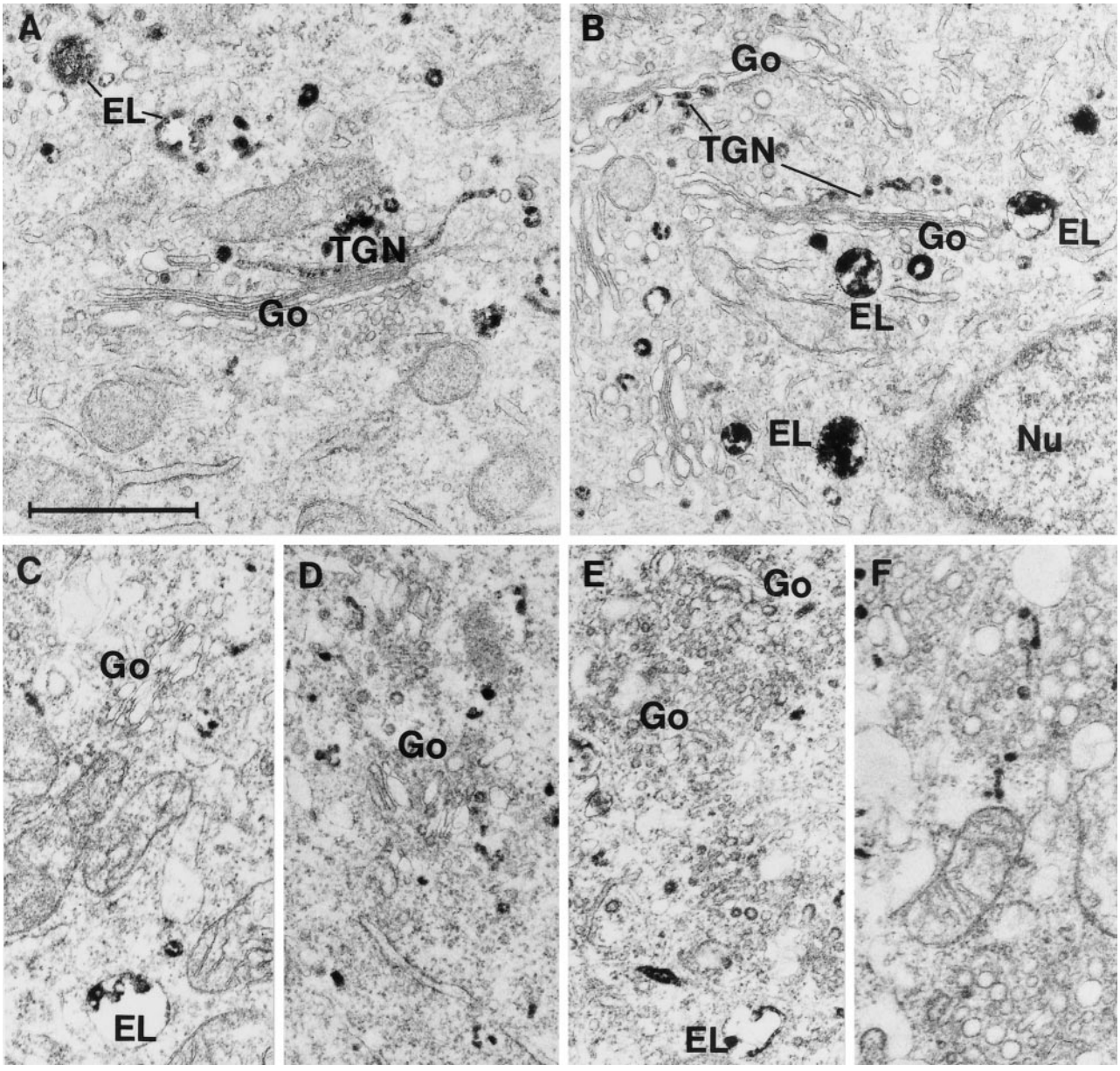

Figure 8. Electron microscopic pictures of HeLa-TetOn/Rab9S21N cells incubated for 2 h at 37°C with a monovalent conjugate of ricin B-chain covalently coupled to HRP. A and B are from control cells, whereas C-F are from cells treated with 5 mM mβCD/chol for 30 min at 37°C before addition of the ricin B-chain conjugate. In control cells, well-developed Golgi stacks (Go) and TGN labeled by ricin B-chain conjugate are seen. In contrast, following incubation with mβCD/chol, the size of distinct Golgi stacks is strongly reduced and numerous small vesicles accumulate instead. EL, ricin B-chain conjugate labeled endosomes/lysosomes; Nu, nucleus; Bar, 1 m.

copy show that increasing the cholesterol content changes the structure of the Golgi apparatus to a more fragmented shape. Thus, this change of the Golgi structure might explain the extensive reduction of ricin transport as well as the reduced sulfation of cellular proteins following treatment with mβCD/chol. A similar change in structure is not observed in cells treated with the concentration of mβCD here used. In contrast, Hansen *et al*. (2000) found that extensive removal of cholesterol by inhibition of cholesterol synthesis followed by high (2% wt/vol) concentrations of mβCD also lead to a change in Golgi morphology. This concentration of mβCD is approximately three times higher than the one we have used in this study. The combined data suggest that a certain level of cholesterol is required to retain the normal structure and function of the Golgi apparatus, as both an increase and a decrease of cholesterol seem to induce fragmentation.

Table 2. The effect of cholesterol depletion on different transport steps. An overview of recent findings

Transport step	Protein/lipid followed	Effect of cholesterol depletion	Reference
Clathrin-dependent endocytosis	Transferrin and EGF	Endocytosis strongly inhibited. Invagination of coated pits perturbed.	(Rodal *et al.*, 1999)
	Transferrin receptor (TR)	Internalization of TR reduced by ~85%. Flattened coated pits.	(Subtil *et al.*, 1999)
Clathrin-independent endocytosis	Ricin	Endocytosis only slightly affected.	(Rodal *et al.*, 1999)
Caveolea	Modified albumins	Endocytosis inhibited, and number of caveolea decreased.	(Schnitzer *et al.*, 1994)
Biogenesis of synaptic-like microvesicles (SLMV)	Synaptophysin and synaptobrevin/VAMP2	SLMV biogenesis blocked	(Thiele *et al.*, 2000)
Recycling from endosomes to cell surface	Transferrin receptor	No effect.	(Subtil *et al.*, 1999)
Plasma membrane to Golgi apparatus	Lactosylceramide (LacCer)	Enhanced targeting of LacCer to the Golgi apparatus	(Puri *et al.*, 1999)
ER to Golgi apparatus	Influenza virus HA and vesicular stomatitis virus glycoprotein (VSVG)	No effect.	(Keller and Simons, 1998)
TGN to apical surface	Influenza virus HA and apical secretory glycoprotein gp-80	Transport step markedly reduced, and substantial missorting to the basolateral surface.	(Keller and Simons, 1998)
	Aminopeptidase N	Enzyme missorted to the basolateral surface. Fragmentation of the Golgi apparatus.	(Hansen *et al.*, 2000)
TGN to the basolateral surface	VSVG	No effect	(Keller and Simons, 1998)
	Na/K-ATPase	No effect	(Hansen *et al.*, 2000)

A number of studies on the effects of decreased cholesterol in various cell types have been summarized in Table 2; and, as shown, depletion of cholesterol inhibits not only invagination of clathrin-coated pits, but also formation of synaptic vesicles (Thiele *et al.*, 2000). It is not clear why cholesterol depletion inhibits formation of only some types of vesicles, but cholesterol might have an effect on membrane curvature that is dependent on neighboring molecules such as glycolipids and cholesterol-binding proteins (Burger, 2000; Keller and Simons, 1998). This might be the reason why reduced transport of the apical marker protein influenza virus hemagglutinin to the cell surface was observed after treatment with mβCD (Keller and Simons, 1998), whereas mβCD had no effect on transport of vesicular stomatitis virus glycoprotein (VSVG-protein) out of the Golgi apparatus. However, it is not necessarily a similar regulation of the transport into and out of the Golgi apparatus.

In Table 3, we have summarized recent results from other laboratories on the effects of increased cholesterol on intracellular transport. An increased cholesterol level in fibroblasts was found to reduce the targeting of the fluorescent analogue of glycosphingolipid lactosylceramide (BODIPY-LacCer) to the Golgi apparatus compared with normal fibroblasts (Puri *et al.*, 1999). Upon increase in the cholesterol level, the BODIPY-LacCer was targeted to the endosomes/lysosomes. The possibility existed that the increased level of cholesterol selectively could affect lipids that might colocalize with cholesterol in rafts. However, as here shown, both transport of the M6PR and transport of ricin, which binds both to glycolipids and glycoproteins, to the Golgi apparatus were strongly decreased by high levels of cholesterol. In contrast to our studies with ricin and mβCD, an enhanced transport of BODIPY-LacCer to the Golgi apparatus was seen in normal fibroblasts depleted for cholesterol. The reason for this difference is not obvious. It should however be noted that the extent of cholesterol depletion and the absolute increase in the cholesterol level might vary in the different studies.

To further investigate the cholesterol dependence of ricin transport to the Golgi apparatus and retrogradely to the ER and the cytosol, we performed a toxicity experiment. Due to the reduced transport of ricin to the Golgi apparatus measured by sulfation and the effect of mβCD/chol on the Golgi structure, one might expect that treatment with both mβCD and mβCD/chol would protect against ricin toxicity and that mβCD/chol would protect to a greater extent than mβCD. However, we found that incubation with mβCD only protected the cells slightly against ricin while the cells were protected two times following incubation with mβCD/chol. A possible explanation for this low protection against ricin is that another step of the retrograde pathway of ricin from endosomes to the ER and the cytosol is facilitated by removal or addition of cholesterol.

After endocytosis, most of the ricin molecules are recycled or transported through the endosomal system to the lysosomes, while a fraction is transported to the Golgi apparatus (van Deurs *et al.*, 1986). Experiments employing TGN38 have shown that transport of proteins from the cell surface to the Golgi apparatus might occur from early endosomes, possibly directly from early endosomes or via the recycling compartment (Mallard *et al.*, 1998; Ghosh *et al.*, 1998; Mallet and Maxfield, 1999). In agreement with this we have recently found that ricin can be transported to the Golgi apparatus by a Rab9-independent pathway (Iversen, Llorente, Nicoziani, van Deurs, and Sandvig, K, unpublished data). We have here investigated the effect of increased and decreased cho-

Table 3. The effect of increased cellular cholesterol on different transport steps. An overview of recent findings

Transport step	Protein/lipid followed	Effect of increased cholesterol	Reference
Plasma membrane to Golgi apparatus	Lactosylceramide (LacCer)	LacCer targeted to endosomes/lysosomes rather than to the Golgi complex.	(Puri *et al.*, 1999)
Late endosomes to TGN	IGF2/MPR	Transport to TGN is inhibited.	(Kobayashi *et al.*, 1999)

lesterol levels on both the Rab9-independent and Rab9-dependent pathways. Measurements of the sulfation of ricin after induced expression of mRab9 and the sulfation of M6PR46HMY enabled us to investigate the two pathways separately. In both instances, extraction of cholesterol from the cells with mβCD strongly reduced sulfation (by ~75%), whereas the sulfation was almost completely inhibited following mβCD/chol treatment. Thus, both pathways are equally sensitive to changes in the cholesterol level. The complete inhibition of sulfation of M6PR46HMY and ricin by treatment with mβCD/chol might be explained by the changed structure of the Golgi apparatus. The inhibition of sulfation of M6PR46HMY in our HeLa cells is in agreement with the results of Kobayashi *et al*. (1999), showing that accumulation of cholesterol in the late endosomes inhibits the transport of the multifunctional receptor IGF2/MPR to TGN. Late endosomes contain a network of lysobisphosphatidic acid-enriched internal membranes (Kobayashi *et al*., 1998), which may participate in regulation of cholesterol transport and thereby endosomal sorting and trafficking (Kobayashi *et al*., 1999).

In conclusion, our results clearly indicate that the right level of cholesterol is essential for efficient endosome to Golgi transport.

ACKNOWLEDGMENTS

We are grateful to Anne-Grethe Myrann, Tove Lie Berle, Mette Ohlsen, Kirsten Pedersen, and Keld Ottosen for their excellent technical assistance. This work was supported by The Norwegian Cancer Society, The Danish Cancer Society, The Danish Medical Research Council, the Novo-Nordisk Foundation, Blix legacy, Torsteds legacy, the Jahre foundation, a NATO Collaborative Research Grant (CRG 900517), a Human Frontier Science Program grant (RG404/96 M), and Jeanette and Søren Bothners legacy.

REFERENCES

Baeuerle, P.A., and Huttner, W.B. (1986). Chlorate: a potent inhibitor of protein sulfation in intact cells. Biochem. Biophys. Res. Commun. *141*, 870–877.

Benting, J.H., Rietveld, A.G., and Simons, K. (1999). N-glycans mediate the apical sorting of a GPI-anchored, raft-associated protein in Madine-Darby canine kidney cells. J. Cell Biol. *146*, 313–320.

Burger, K.N.J. (2000). Greasing membrane fusion and fission machineries. Traffic *1*, 605–613.

Ciechanover, A., Schwarts, A.L., Dautry-Varsat, A., and Lodish, H.F. (1983). Kinetics of internalization and recycling of transferrin and the transferrin receptor in a human hepatoma cell line. J. Biol. Chem. *258*, 9681–9689.

Fraker, P.J., and Speck, J.C. (1978). Protein and cell membrane iodinations with a sparingly soluble chloroamide, 1,3,4,6-tetrachloro-3a,6a-diphenylglycoluril. Biochem. Biophys. Res. Commun. *80*, 849–857.

Ghosh, R.N., Mallet, W.G., Soe, T.T., McGraw, T.E., and Maxfield, F.R. (1998). An endocytosed TGN38 chimeric protein is delivered to the TGN after trafficking through the endocytotic recycling compartment in CHO cells. J. Cell Biol. *142*, 923–936.

Hailstones, D., Sleer, L.S., Parton, R.G., and Stanley, K.K. (1998). Regulation of caveolin and caveolae by cholesterol in MDCK cells. J. Lipid Res. *39*, 369–379.

Hansen, G.H., Niels-Christiansen, L.-L., Thorsen, E., Immerdal, L., and Danielsen, E.M. (2000). Cholesterol depletion of enterocytes. J. Biol. Chem. *275*, 5136–5142.

Harder, T., and Simons, K. (1997). Caveolae, DIGs, and the dynamics of sphingolipid-cholesterol microdomains. Curr. Opin. Cell Biol. *9*, 534–542.

Itin, C., Rancaño, C., Nakajima, Y., and Pfeffer, S.R. (1997). A novel assay reveals a role for soluble N-Ethylmaleimide-sensitive fusion attachment protein in mannose 6-phosphate receptor transport from endosomes to the trans Golgi network. J. Biol. Chem. *272*, 27737–27744.

Keller, P., and Simons, K. (1998). Cholesterol is required for surface transport of influenza virus hemagglutinin. J. Cell Biol. *140*, 1357–1367.

Klein, U., Gimpl, G., and Fahrenholz, F. (1995). Alteration of the myometrial plasma membrane cholesterol content with b-cyclodextrin modulates the binding affinity of the oxytocin receptor. Biochemistry *34*, 13784–13793.

Kobayashi, T., Beuchat, M.-H., Lindsay, M., Frias, S., Palmiter, R.D., Sakuraba, H., Parton, R.G., and Gruenberg, J. (1999). Late endosomal membranes rich in lysobisphosphatidic acid regulate cholesterol transport. Nat Cell Biol. *1*, 113–118.

Kobayashi, T., Stang, E., Fang, K.S., de Moerloose, P., Parton, R.G., and Gruenberg, J. (1998). A lipid associated with the antiphospholipid syndrome regulates endosome structure and function. Nature *392*, 193–197.

Laemmli, U.K. (1970). Cleavage of structural proteins during the assembly of the head of bacteriophage T4. Nature *227*, 680–685.

Mallard, F., Antony, C., Tenza, D., Salamero, J., Goud, B., and Johannes, L. (1998). Direct pathway from early/recycling endosomes to the Golgi apparatus revealed through the study of shiga toxin B-fragment transport. J. Cell Biol. *143*, 973–990.

Mallet, W.G., and Maxfield, F.R. (1999). Chimeric forms of furin and TGN38 are transported from the plasma membrane to the trans-Golgi network via distinct endosomal pathways. J. Cell Biol. *146*, 345–359.

Mayor, S., Sabharanjak, S., and Maxfield, F.R. (1998). Cholesterol-dependent retention of GPI-anchored proteins in endosomes. EMBO J. *17*, 4626–4638.

Mukherjee, S., and Maxfield, F.R. (1999). Cholesterol: stuck in traffic. Nat. Cell Biol. *1*, 37–38.

Olsnes, S., van Deurs, B., and Sandvig, K. (1993). Protein toxins acting on intracellular targets: cellular uptake and translocation to the cytosol. Med. Microbiol. Immunol. *182*, 51–61.

Puri, V., Watanabe, R., Dominguez, M., Sun, X., Wheatley, C.L., Marks, D.L., and Pagano, R.E. (1999). Cholesterol modulates membrane traffic along the endocytic pathway in sphingolipid-storage diseases. Nat. Cell Biol. *1*, 386–388.

Rapak, A., P.Ø. Falnes, and S. Olsnes. (1997). Retrograde transport of mutant ricin to the endoplasmic reticulum with subsequent translocation to cytosol. Proc. Natl. Acad. Sci. USA *94*, 3783–3788.

Riederer, M.A., Soldati, T., Shapiro, A.D., Lin, J., and Pfeffer, S.R. (1994). Lysosome biogenesis requires rab9 function and receptor recycling from endosomes to the trans-Golgi network. J. Cell Biol. *125*, 573–582.

Rodal, S.K., G. Skretting, Ø. Garred, F. Vilhardt, B. van Deurs and K. Sandvig (1999). Extraction of cholesterol with methyl-b-cyclodextrin perturbs formation of clathrin-coated endocytic vesicles. Mol. Biol. Cell *10*, 961–974.

Rothberg, K.G., Ying, Y.-S., Kamen, B.A., and Anderson, R.G.W. (1990). Cholesterol controls the clustering of the glycophospholipid-anchored membrane receptor for 5-methyltetrahydrofolate. J. Cell Biol. *111*, 2931–2938.

Sandvig, K., and Olsnes, S. (1979). Effect of temperature on the uptake, excretion and degradation of abrin and ricin by HeLa cells. Exp. Cell Res. *121*, 15–25.

Sandvig, K., Olsnes, S., Petersen, O.W., and van Deurs, B. (1987). Acidification of the cytosol inhibits endocytosis from coated pits. J. Cell Biol. *105*, 679–689.

Sandvig, K., and van Deurs, B. (1996). Endocytosis, intracellular transport, and cytotoxic action of shiga toxin and ricin. Physiol. Rev. *76*, 949–966.

Sandvig, K., and van Deurs, B. (1999). Endocytosis and intracellular transport of ricin: recent discoveries. FEBS Letters *452*, 67–70.

Schnitzer, J.E., Oh, P., Pinney, E., and Allard, J. (1994). Filipin-sensitive caveolae-mediated transport in endothelium: reduced transcytosis, scavenger endocytosis, and capillary permeability of select macromolecules. J. Cell Biol. *127*, 1217–1232.

Simons, K., and Ikonen, E. (1997). Functional rafts in cell membranes. Nature *387*, 569–572.

Simpson, J.C., Dascher, C., Roberts, L.M., Lord, J.M., and Balch, W.E. (1995). Ricin cytotoxicity is sensitive to recycling between the endoplasmic reticulum and the Golgi complex. J. Biol. Chem. *270*, 20078–20083.

Subtil, A., Gidarov, I., Kobylarz, K., Lampson, M.A., Keen, J.H., and McGraw, T.E. (1999). Acute cholesterol depletion inhibits clathrin-coated pit budding. Proc. Natl. Acad. Sci. USA *96*, 6775–6780.

Thiele, C., Hannah, M.J., Fahrenholz, F., and Huttner, W.B. (2000). Cholesterol binds to synaptophysin and is required for biogenesis of synaptic vesicles. Nat. Cell Biol. *2*, 42–49.

van Deurs, B., Sandvig, K., Petersen, O.W., Olsnes, S., Simons, K., and Griffiths, G. (1988). Estimation of the amount of internalized ricin that reaches the trans-Golgi network. J. Cell Biol. *106*, 253–267.

van Deurs, B., Tønnessen, T.I., Petersen, O.W., Sandvig, K., and Olsnes, S. (1986). Routing of internalized ricin and ricin conjugates to the Golgi complex. J. Cell Biol. *102*, 37–47.

Wales, R., Roberts, L.M., and Lord, J.M. (1993). Addition of an endoplasmic reticulum retrieval sequence to ricin A chain significantly increases its cytotoxicity to mammalian cells. J. Biol. Chem. *268*, 23986–23990.

Wesche, J., Rapak, A., and Olsnes, S. (1999). Dependence of ricin toxicity on translocation of the toxin A-chain from the endoplasmic reticulum to the cytosol. J. Biol. Chem. *274*, 34443–34449.